Characterization of Microporosity in Ordered Mesoporous Material MAS-7 by ^{129}Xe NMR Spectroscopy

Fang Chen,[†] Mingjin Zhang,[†] Yu Han,[‡] Fengshou Xiao,[‡] Yong Yue,*[,†] Chaohui Ye,[†] and Feng Deng*[,†]

State Key Laboratory of Magnetic Resonance and Atomic and Molecular Physics, Wuhan Institute of Physics and Mathematics, The Chinese Academy of Sciences, Wuhan 430071, P. R. China, and Department of Chemistry and State Key Laboratory of Inorganic Synthesis and Preparative Chemistry, Jilin University, Changchun 130023, P. R. China

Received: October 24, 2003

A new kind of ordered mesoporous aluminosilicate material MAS-7, containing micropores inside its pore walls, has been investigated by ^{129}Xe NMR spectroscopy as a function of xenon pressure over a wide range of temperatures. ^{129}Xe NMR results reveal that two different independent micropore systems are present in the mesoporous walls of MAS-7. Two signals are observed in the ^{129}Xe NMR spectra, which can be attributed to two kinds of fast exchange of xenon atoms in the two different types of micropores (micropores I and II) with those in the mesopores and in the interparticle space of MAS-7. Coadsorption experiments of xenon and guest molecules with different sizes provide an estimation of the sizes of micropores in MAS-7. Micropore I has a diameter of ca. 0.74 nm, which is most likely formed by the primary structure units of zeolite beta. Micropore II possesses a relatively small pore diameter of 0.44−0.49 nm, which may be generated from partial occlusion of triblock polymer (template used in the synthesis of MAS-7) chains into the mesoporous walls of MAS-7. The details of xenon adsorption and motion are also thoroughly studied by variable-temperature (VT) ^{129}Xe NMR experiments. The VT ^{129}Xe NMR experiments suggest that even bulk (solid or liquid) xenon atoms probably formed on the mesoporous wall still undergo fast exchange with xenon in the other adsorption states (such as xenon in the micropores) at 124 K, indicating there is a good communication among the various types of pores in MAS-7.

Introduction

As is well-known, the versatile zeolites, such as Y and ZSM-5, which have uniform and molecular size pores, high stability, and strong acidity, are widely used as adsorbents or catalysts in the chemical and the petrochemical industry. However, they cannot effectively catalyze large molecules due to the restriction of microporous size.[1,2] The synthesis of mesoporous silicate materials, such as MCM-41,[3,4] provides a potential for the materials as versatile catalysts and catalyst support for conversion of large molecules. MCM-41 (a member of the M41S family) synthesized with surfactant molecules as a structure-directing reagent possesses a hexagonal arrangement of uniformly sized mesopores with diameters in the range 1.5−10 nm. The pore sizes can be adjusted by changing the length of the alkyl chains of the surfactant molecules. The resultant mesoporous materials are characterized by long-range periodicity in the arrangements of pores with locally disordered inorganic frameworks. Generally, incorporation of heteratoms such as Al into the siliceous mesoporous materials will introduce a charge imbalance in the framework which is balanced by protons, thus generating Brönsted acidity on these materials. However, as compared with conventional zeolites, these mesostructured materials have relatively weak acidity and low hydrothermal stability,[5] which may probably limit their practical application in catalytic reactions. The relatively low acidity of the mesoporous materials may be attributed to the amorphous nature of their pore walls and the special nature of acid sites.[5]

To expand the commercial applications of mesoporous materials, many effects have been made to improve the acidity and the hydrothermal stability of MCM-41 or to prepare other stable and high acidic mesoporous materials.[6−19] SBA-15, a new type of well-ordered hexagonal mesoporous molecular sieve with thicker walls and much higher hydrothermal stability than MCM-41, was prepared by using triblock copolymer as templates.[9] Stable aluminosilicate mesostructures were also successfully prepared from nanoclustered zeolite seeds under alkaline or strongly acidic conditions.[16,17] More recently, a new mesoporous material designated as MAS-7 was synthesized by using triblock polymers in strongly acidic conditions by a two-step procedure.[19] First, precursors containing zeolite nanoclusters (primary structure units of zeolite) were prepared. Second, the preformed precursors were used to assemble mesoporous material with triblock copolymers in strong acidic media. In this way, the heteroatoms (such as Al) were fixed in the framework of the zeolite nanoclusters in the first step and then directly introduced into the mesoporous structure in the second step. The resulting material shows an ordered hexagonal mesoporous structure with much thicker walls than MCM-41, consisting of micropores in its pore walls that are probably formed by the primary structure units of zeolite. This material also shows high catalytic activities for the cracking of both small and large organic molecules because it contains the benefits of both mesoporous materials and microporous zeolites. Although

[†] Wuhan Institute of Physics and Mathematics.
[‡] Jilin University.
* Corresponding authors: e-mail dengf@wipm.ac.cn (Fax: 86-27-87199291) and yueyong@wipm.ac.cn.

10.1021/jp031187u CCC: $27.50
Published on Web 03/02/2004

TABLE 1: Some Properties of MAS-7, SBA-15, MCM-41, and Zeolite Beta Obtained from XRD and N_2 Adsorption Measurements

sample	BET surface area (m^2/g)	total pore volume (cm^3/g)	micropore volume (cm^3/g)	mesopore or micropore size (nm)	wall thickness (nm)	Si/Al
MAS-7	980	1.15	0.15	7.6	5.4	30
SBA-15	870	1.29	0.05	7.6	3.2	∞
MCM-41	800	0.63		2.7	1.9	∞
zeolite beta	396	0.19	0.19	0.77		30

nanoranged ordered microporoes seem to be found within the pore walls of MAS-7 via high-resolution transmission electron microscopy (HRTEM) and N_2 adsorption isotherm,[19,20] the detailed structure and properties of the micropores (such as their distribution and connectivity, the adsorption, and diffusion of guest molecules inside the micropores) are still poorly understood.

^{129}Xe NMR spectroscopy is an important and very useful technique for investigating the pore structure of porous materials. ^{129}Xe is an inert, nonpolar, spherical atom with a large electron cloud sensitive to its environments and interactions, which results in a wide ^{129}Xe NMR chemical shift range. Together with a nuclear spin $^1/_2$ and a relatively high NMR sensitivity, ^{129}Xe is very suitable as an ideal NMR probe. In the past 20 years, ^{129}Xe NMR of adsorbed xenon has proved to be a valuable tool for investigating a variety of porous materials,[22−34] such as zeolites, mineral clay, mesoporous materials, carbon nanotubes, and so forth. For xenon adsorbed in a porous material, the observed ^{129}Xe NMR chemical shift is the weighted average of different types of interactions on the NMR time scale. In particular, for xenon adsorbed on zeolites at room temperature, Ito and Fraissard suggested that the chemical shift of adsorbed xenon is the sum of several terms corresponding to the various perturbations it suffers.[22,23]

$$\delta = \delta_0 + \delta_S + \delta_{Xe-Xe}\rho_{Xe} + \delta_E + \delta_M + \delta_{SAS} \qquad (1)$$

where δ_0 is the reference chemical shift, $\delta_{Xe-Xe}\rho_{Xe}$ arises from Xe−Xe collisions and is expected to vary linearly with xenon density at low xenon loading, δ_E is the shift due to the electric field caused by cations, δ_M is an extra term accounting for the presence of paramagnetic species, δ_{SAS} is the shift due to strong adsorption sites, and δ_S is the shift due to interaction of Xe with the pore surface, which is related to the dimension and shape of the pore by means of the mean free path $\bar{l}$ of adsorbed Xe in the pore. The δ_S against $\bar{l}$ shows a hyperbolic relation:[24]

$$\delta_S = 243\frac{2.054}{2.054 + \bar{l}} \qquad (2)$$

Generally, the larger the pore size, the smaller the value of δ_S. However, this empirical relationship does not fit for mesoporous materials. In contrast to zeolites, the chemical shift of xenon adsorbed in mesoporous materials is roughly independent of xenon pressure and usually shows unexpectedly large value.[25−28] There is no a unique correlation that fits all mesoporous materials, and the observed ^{129}Xe chemical shift strongly depends on the synthesis conditions of mesoporous materials.[25−28] This is at least partly due to the amorphous nature of the pore wall, the presence of micropores, or structure defects in mesoporous materials.[26−28] Especially, the presence of micropores in mesoporous materials significantly affects the chemical shift of adsorbed xenon.[28]

In this work, we attempted to characterize the microporosity in MAS-7 by ^{129}Xe NMR spectroscopy. Consequently, we measured ^{129}Xe NMR spectra with different xenon pressure over a wide temperature range. In addition, coadsorption of Xe and guest molecules with different sizes was also studied in order to estimate the size of micropores in MAS-7.

Experimental Section

Sample Preparation. MAS-7 was hydrothermally synthesized from an assembly of triblock polymers (Pluronic P123) with preformed zeolite beta precursors in a strong acidic media by a two-step procedure. The details of synthesis procedure and the results of structural characterization by other analytical techniques have been previously published.[19−21] The XRD pattern suggested that well-ordered arrays of mesopores with uniform pore size were formed, and no other impurity was present in MAS-7. For comparison, mesoporous materials MCM-41, SBA-15, and zeolite beta samples were synthesized according to the literature.[3,4,9,35,36] The results obtained from XRD and N_2 sorption measurements are listed in Table 1.

Dehydrated samples for ^{129}Xe NMR measurement were prepared as follows. A known amount of the samples (such as MAS-7, SBA-15, or MCM-41) was placed in a glass tube with a 8 mm outside diameter. The tube was connected to a vacuum line. The temperature was gradually increased at a rate of 1 °C min^{-1}, and the sample was kept at final temperature of 300 °C at a pressure below 10^{-3} Pa over a period of 12 h and then cooled. After the sample cooled to ambient temperature, a measured volume of Xe gas (^{129}Xe 26.44%) with a known pressure was condensed and frozen inside the sample by cooling the sample region of the glass tube with liquid nitrogen. Finally, the tube was flame-sealed. For ^{129}Xe VT experiment, approximately 1.5×10^3 Pa of He (99.995%) was also introduced into the corresponding samples in order to increase the rate of heat transfer and avoid the effect of temperature gradient during the VT experiment.

The samples of coadsorption of Xe and guest molecules were prepared in a similar manner. After the sample dehydration, a known amount of guest molecules was first introduced, and then gaseous xenon was frozen onto the sample with liquid N_2. Before NMR measurements, the samples were kept at room temperature for several days in order to avoid macroscopic heterogeneous distribution of adsorbed molecules in the samples.

To obtain samples with different water uptakes, hydrated MAS-7 samples were outgassed on a vacuum line for different periods of time at room temperature, and then gaseous xenon was introduced.

Room temperature (RT) ^{129}Xe NMR spectra were acquired using a Varian 200 spectrometer modified with a Tecmag system at a frequency of 55.34 MHz. A 5 μs ($\pi/4$) excitation pulse and a 1−4 s recycle delay were employed to record ^{129}Xe NMR spectra. Variable temperature (VT) experiments were carried out on a Bruker WP-80 spectrometer at a frequency of 22.17 MHz with a 6 μs ($\pi/4$) excitation pulse and a 1 s recycle delay. The samples were cooled or warmed in steps from RT to the expected temperature at a rate of approximately 1−2 K/min, being allowed to equilibrate at a desired temperature for 10−20 min before data acquisition.

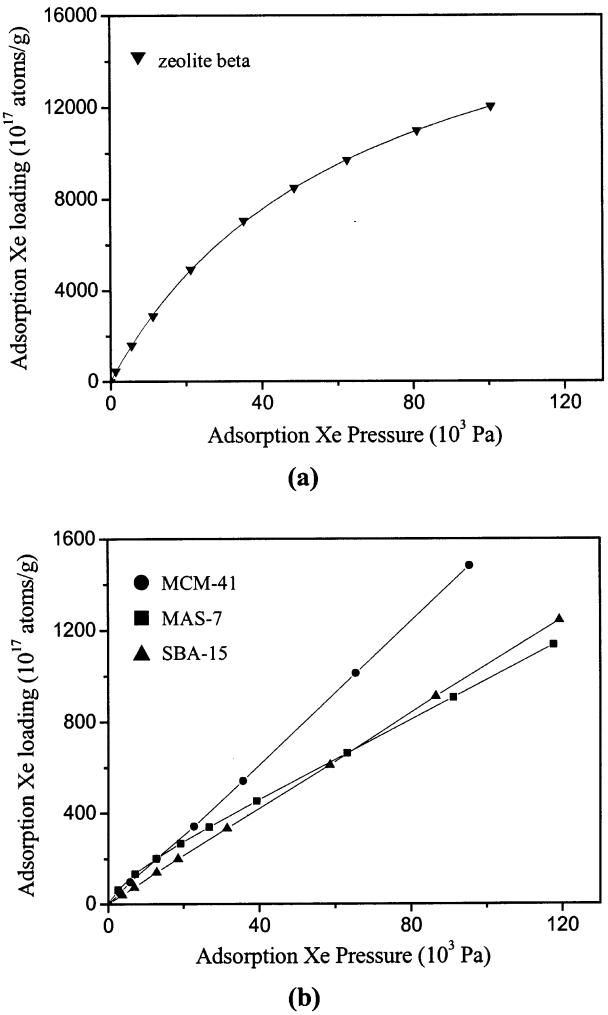

Figure 1. Adsorption isotherms of xenon in (a) zeolite beta and (b) MCM-41, MAS-7, and SBA-15 at 295 K.

We measured the ^{129}Xe chemical shift, at room temperature, of an external standard sample of Xe gas at 6.3 atm with a small amount of oxygen prior to each set of measurements. The shift was then corrected to zero pressure with the equations given by Jameson et al.[37,38]

Results and Discussion

Adsorption Isotherm of Xenon. The adsorption isotherms of xenon at 295 K in zeolite beta, MCM-41, SBA-15, and MAS-7 are shown in Figure 1, which were obtained by a volumetric method. The adsorption isotherm of xenon in zeolite beta shows a Langmuir-type isotherm that is usually observed for microporous materials and can be described by a Langmuir-type equation:

$$N = n_a \frac{k_1 P}{1 + k_1 P} \tag{3}$$

where N is the xenon loading at a pressure P, n_a ($(1.98 \pm 0.02) \times 10^{21}$ atoms g^{-1}) is the adsorption capacity, and k_1 ($(1.55 \pm 0.02) \times 10^{-5}$ Pa^{-1}) is the Langmuir adsorption constant. On the contrary, the adsorption isotherm of xenon in mesoporous material MCM-41 exhibits a linear correlation over a wide range of xenon pressures (Henry-type isotherm). The adsorption of xenon in mesoporous material MAS-7 shows a Langmuir-type isotherm at low pressure while a Henry-type isotherm at high pressure, which can be described by the following equation:

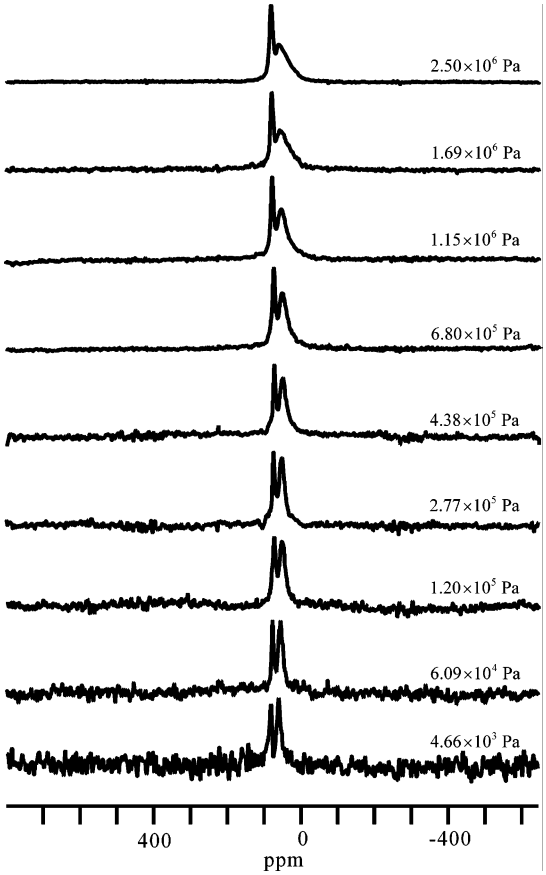

Figure 2. Pressure-dependent ^{129}Xe NMR spectra (acquired at room temperature) of xenon adsorbed in MAS-7.

$$N = n_1 \frac{k_1 P}{1 + k_1 P} + K_2 P \tag{4}$$

where K_2 is the Henry adsorption constant. Obviously, the adsorption isotherm of xenon in MAS-7 indicates the presence of some micropores inside the material, which are first occupied by xenon atoms. This is consistent with the result obtained by the N_2 adsorption isotherm.[19] For SBA-15, no obvious Langmuir-type adsorption isotherm was observed, probably due to the low amount of micropores in the material.

Room Temperature ^{129}Xe NMR. Figure 2 shows the ^{129}Xe NMR spectra of xenon adsorbed in MAS-7 with adsorption pressure of xenon varying from 4.66×10^3 to 2.50×10^6 Pa. No ^{129}Xe signal arising from free xenon gas can be observed, which is likely due to the rapid exchange between xenon atoms in the interparticle space and those in the pores of MAS-7. Two well-resolved resonances at about 75 ppm (line a) and 53 ppm (line b) are observed in the ^{129}Xe spectra acquired at RT, while only a single resonance is present in the ^{129}Xe NMR spectra of SBA-15 and MCM-41 within a large range of xenon pressure (not shown). The chemical shifts of the two signals follow a parabolic correlation against the adsorption pressure of xenon (see Figure 3): an initial decrease, reaching a minimum with a xenon pressure of ca. 2.5×10^5 Pa, and then a slow increase. The chemical shifts (δ_s) extrapolated to zero xenon loading are about 81 and 60 ppm for line a and line b, respectively. In the case of xenon adsorbed in zeolite, a parabolic correlation is usually ascribed to the presence of strong adsorption sites or divalent cations. Since no divalent cations were involved in the synthesis of MAS-7 and the ^{27}Al NMR spectroscopy revealed

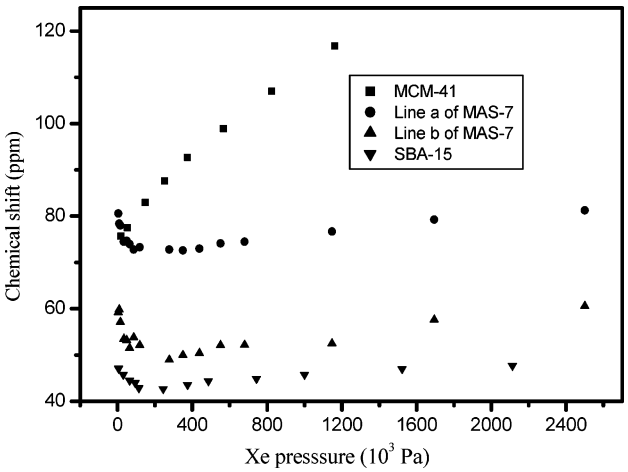

Figure 3. Variation of ^{129}Xe NMR chemical shift vs adsorption pressure of xenon at room temperature: ■, MCM-41; ●, line a of MAS-7; ▲, line b of MAS-7; ▼, SBA-15.

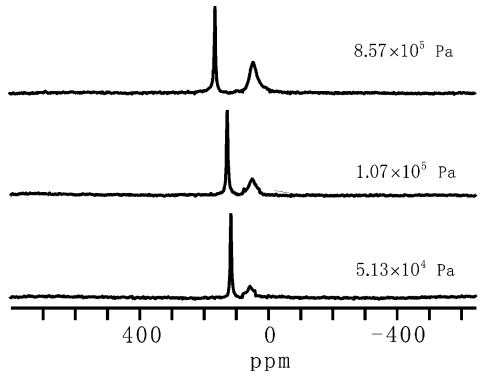

Figure 4. Pressure-dependent ^{129}Xe NMR spectra of xenon adsorbed in a 1:1 beta zeolite/MCM-41 mixture at room temperature.

that the heteroatoms of Al were effectively incorporated into the framework of MAS-7,[19] the effect of electric field on the ^{129}Xe chemical shift arising from the divalent cations can be neglected, and the parabolic correlation in MAS-7 is most likely due to the presence of strong adsorption sites. The parabolic correlation between the ^{129}Xe NMR chemical shifts and xenon pressure can also be observed for the SBA-15 sample, while a linear correlation is present for the MCM-41 sample. As is well-known, SBA-15 is a typical mesoporous materials containing micropores inside its pore walls, whereas almost no micropores are present in the walls of MCM-41 materials. Furthermore, no obvious signal can be detected in the ^{129}Xe spectrum of a MCM-41 sample with a low xenon adsorption pressure (4.66×10^3 Pa) under the same acquisition condition. Therefore, we suspect that the parabolic correlation observed for the MAS-7 sample should arise from the presence of micropores as strong adsorption sites in the mesoporous MAS-7. For xenon adsorbed in microporous materials, a smaller pore size usually leads to a larger ^{129}Xe chemical shift at a low xenon loading. It seems that the downfield signal can be assigned to xenon in the micropores and the upfield signal to xenon in the mesopores of MAS-7. However, at present, we are unable to give a definite assignment for the two ^{129}Xe signals.

In the synthesis of MAS-7, zeolite beta precursors (primary structure units) were used to assemble mesoporous framework. For comparison, we recorded ^{129}Xe NMR spectra of xenon adsorbed in a mixture of MCM-41 and zeolite beta (1:1) at room temperature (see Figure 4). Two individual peaks are observed and the ^{129}Xe chemical shift of downfield signal (arising from Xe in zeolite beta) increases, while that of the upfield signal (due to Xe in MCM-41) slightly decreases with the increase of xenon pressure. On the other hand, it can be seen from Figure 4 that the relative integrated intensity of the upfield signal gradually increases, while that of the downfield signal remains almost unchanged with increasing xenon pressure, which can be contributed to the difference of the xenon sorption isotherms between zeolite beta and MCM-41 as shown in Figure 1. The xenon sorption isotherms for zeolite beta quickly approach saturation as xenon pressure increases, but for xenon adsorbed in mesoporous materials, such as MCM-41, the adsorption pressure for saturation is much larger than that in zeolite beta. The integrated intensities of the two peaks reflect that the relative uptake of xenon adsorbed in zeolite beta (micropores) and MCM-41 (mesopores). It looks like that xenon atoms are preferentially adsorbed in the micropores of zeolite beta, especially at low xenon pressure. Obviously, the variations of the chemical shift and the integrated intensities of the two signals are quite different from those for the line a and line b observed in the ^{129}Xe NMR spectra of MAS-7. Therefore, we are inclined to assign the two signals in the ^{129}Xe NMR spectra of MAS-7 to xenon adsorbed in two types of micropores rather than xenon in micropores and mesopores. We denote the micropores corresponding to line a and line b as "micropore I" and "micropore II", respectively. Xenon atoms in the two types of micropores may probably undergo fast exchange with those in the void of mesoporoes. However, they exchange slowly between themselves within the NMR time scale. The chemical shifts of the two signals are an average of the shifts of xenon in the micropores and mesopores of MAS-7. The observation of two separate resonances over a wide range of xenon pressure also suggests that there is no direct communication between the two different types of micropores. That is to say, they are independent pore systems.

Coadsorption Experiments. Under fast exchange conditions, the observed chemical shift is the weighted average value of the shifts of xenon in the micropore and mesopore, which can be expressed as follows:

$$\delta_{\text{obs}} = \frac{N_1}{N}\delta_1 + \frac{N_2}{N}\delta_2 \qquad (5)$$

where δ_{obs} is the observed chemical shift in MAS-7; δ_1 and δ_2 ($\delta_1 > \delta_2$) are the chemical shifts of xenon adsorbed in the micropores and mesopores of MAS-7, respectively, N is the total number of xenon adsorbed in MAS-7, and N_1 and N_2 are the populations of xenon adsorbed in the micropores and mesopores, respectively. Considering eq 5, one can find that if the proportion of xenon adsorbed in micropores and mesopores is varied, the observed chemical shift must be changed. A decrease in the proportion of xenon in micropores will cause a decrease in the observed chemical shift when δ_1 is much larger than δ_2. Adsorption of different sizes of guest molecules in microporous materials is a conventional technique for estimating the micropore sizes. Small molecules preferentially trapped in micropores can reduce the proportion of xenon in these pores, which will lead to a decrease in the observed ^{129}Xe NMR chemical shift. To confirm this assumption, several guest molecules with different sizes are adsorbed in MAS-7. After coadsorption of xenon and water molecule in MAS-7, a significant decrease (ca. 25 ppm) in the ^{129}Xe chemical shift of the two signals is observed in the hydrated sample of MAS-7 (see Figure 5), which depends on the loading of water molecules. The more the water molecules are trapped in MAS-7, the more the decrease in the ^{129}Xe chemical shift. The result is quite

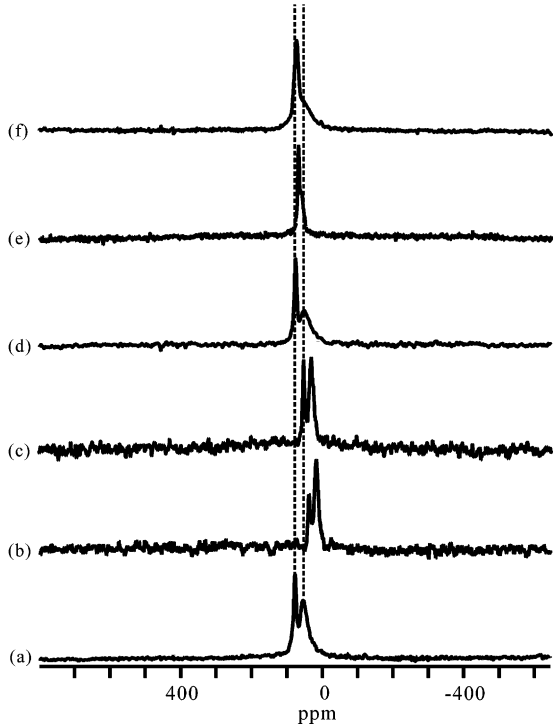

Figure 5. Room temperature (RT) ^{129}Xe NMR spectra of xenon adsorbed in (a) dehydrated MAS-7, (b) hydrated MAS-7 with 1 h outgassed at RT, (c) hydrated MAS-7 with 1.5 h outgassed at RT, (d) hydrated MAS-7 with 4 h outgassed at RT, (e) dehydrated MAS-7 with a benzene loading of 6.1×10^{-4} mol/g, and (f) dehydrated MAS-7 with a 1,3,5-triisopropylbenzene (TIPB) loading of 3.2×10^{-4} mol/g.

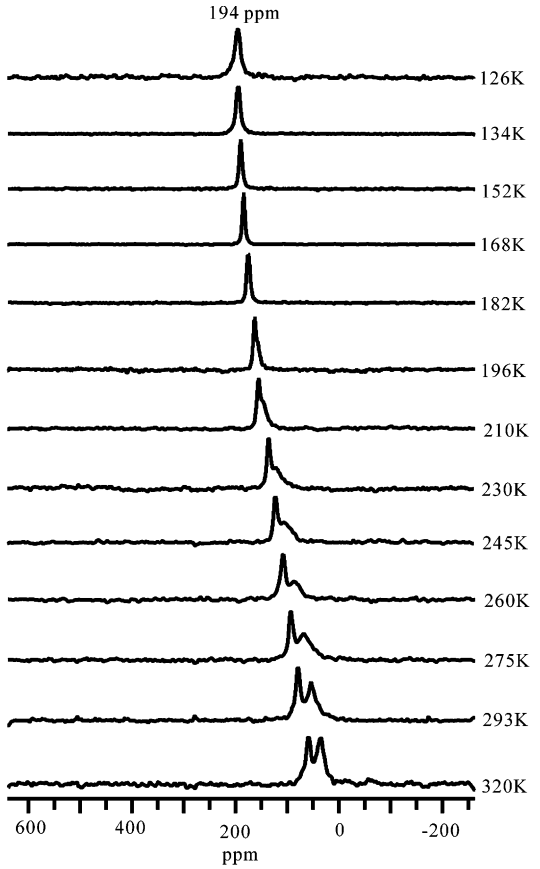

Figure 6. Temperature-dependent ^{129}Xe NMR spectra of xenon adsorbed in MAS-7 with a xenon pressure of 6.3×10^5 Pa. The temperature was varied from 126 to 320 K.

different from the cases of xenon adsorbed in hydrated mesoporous silica[29] or microporours materials (such as zeolite NaY),[30] where an increase in ^{129}Xe chemical shift was always observed. In these cases, occupation of water molecules in the mesopores or micropores decreases the mean free path of xenon, resulting in an increase in the corresponding ^{129}Xe chemical shifts. For a hydrated MCM-41 material with roughly internal surfaces,[27] a decrease in chemical shift was also observed, while several ^{129}Xe signals probably due to heterogeneous adsorption of water on the surface were observed and their corresponding ^{129}Xe chemical shifts remain almost unchanged with increasing water loading. The difference between MAS-7 and MCM-41 may arise from a good communication among the pore systems of MAS-7. In MCM-41, the mesopore wall is a barrier for guest molecules, and adsorbed molecules in one mesopore cannot directly get into another neighboring mesopore though the pore wall. As a result, xenon atoms adsorbed in different adsorption zones remain their local characteristics, and the chemical shifts do not change with the water loading. However, since micropores are present in the pore wall of MAS-7, the small molecules (such as xenon and water) adsorbed in one mesopore can easily pass through the pore wall that contains two types of micropores to another neighboring mesopore. Obviously, MAS-7 shows a much better communication for adsorbed molecules than MCM-41. The exchange of xenon adsorbed in the different adsorption zones is much more efficient than that in MCM-41.

After coadsorption of xenon and benzene (with a kinetic diameter of 0.49 nm[39]), the ^{129}Xe NMR chemical shift of the downfield signal is decreased by ca. 10 ppm while that of the upfield signal remains almost unchanged, indicating that benzene molecules can penetrate into micropore I, while micropore II is not accessible to benzene molecules. In the case of coadsorption of xenon and 1,3,5-triisopropylbenzene (TIPB) (with a kinetic diameter 0.74 nm[39]), we observed a much smaller decrease (ca. 3 ppm) in the chemical shift of the downfield signal and a decrease in the integrated intensity of upfield signal, suggesting that only a small amount of TIPB molecules can get into micropore I while micropore II is not accessible to TIPB. On the basis of the coadsorption experiments, it can be estimated that the size of micropore I is close to 0.74 nm and that of micropore II is in the range 0.44−0.49 nm.

VT ^{129}Xe NMR. Temperature-dependent ^{129}Xe NMR spectra of samples with low xenon pressures ($<10^6$ Pa) are similar. Figure 6 shows a typical result for a sample with a xenon pressure of 6.3×10^5 Pa. When the temperature decreases from 320 to 196 K, the two peaks shift to downfield and move close to each other, and the intensity of the downfield signal partially increases at the expense of the upfield signal, owning to a redistribution of Xe between the different types of adsorption environments. At 182 K, the two components coalesce to one single line. Further decreasing temperature causes a further increase in the chemical shift (194 ppm at 126 K). It is clear that with lowering temperature the concentration of xenon in both the micropores and the mesopores of MAS-7 increases, while that in the interparticle space decreases.[31] Most likely, for the xenon atoms in the mesopores of MAS-7, they spend more time in the potential well associated with the mesoporous wall at low temperature,[32] which will accelerate the exchange of xenon in the two different types of micropores with xenon near mesoporous wall. Eventually, the indirect exchange of xenon bewteen the two different types of micropores through xenon atoms near the mesoporous wall is considerably increased. As a result, only one symmetrical resonance is observed at temperature below 196 K.

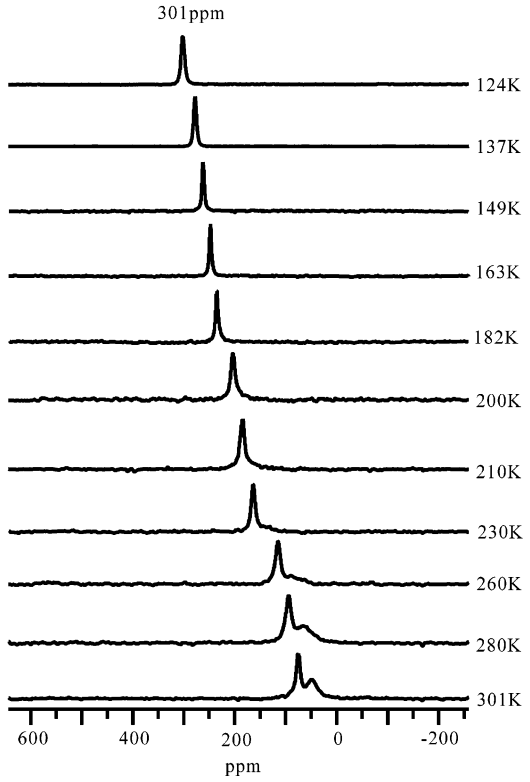

Figure 7. Temperature-dependent ^{129}Xe NMR spectra of xenon adsorbed in MAS-7 with a xenon pressure of 2.0×10^6 Pa. The temperature was varied from 124 to 301 K.

Figure 7 shows the VT ^{129}Xe NMR spectra of MAS-7 with a high xenon pressure (2.0×10^6 Pa). Two separate resonances are observed when temperature is above 230 K, while only a symmetrical resonance is present when temperature is reduced from 230 to 124 K. The appearance of single resonance at low temperature can be attributed to the fast exchange of xenon among the different adsorption zones. It is noteworthy that the observed chemical shift increases with decreasing temperature and can reach 262 ppm (the chemical shift range of liquid xenon) at 149 K and 301 ppm (the chemical shift range of solid xenon) at 124 K, indicating that phase transitions of xenon probably occur. As is well-known, the phase transition of xenon is a cooperative phenomenon requiring the participation of many atoms, and Monte Carlo calculations have proved that a xenon phase transition requires a cluster having at least 13 xenon atoms.[40] Because of the restriction of pore size, only a finite number of xenon atoms are trapped inside the micropore of zeolite; in general, only bulk liquid xenon can be formed, and liquid−solid transition cannot occur inside micropores even at very low temperature. For example, Cheung et al.[33] found that the supercage in Y zeolite (with a free diameter of 1.3 nm and a pore opening of 0.74 nm) could hold between 10 and 11 xenon atoms and bulk liquid xenon formed in the supercage had a chemical shift of 250−270 ppm, while bulk solid xenon condensed on the exterior surface of Y zeolite gave rise to a chemical shift of 304 ppm. Since the sizes of the two types of micropores in MAS-7 are much smaller than that of the supercage in Y zeolite, we suspect that the phase transition of xenon most likely proceeds on the mesoporous wall of MAS-7. It is interesting that only one resonance line is present over a wide temperature range, implying that even the bulk (solid or liquid) xenon still undergoes fast exchange with xenon in the other adsorption states (such as xenon in the micropores) of MAS-7 at 124 K. This is quite different from the case of mesoporous silica,[29] where two separate signals from liquid and solid xenon could be simultaneously observed in the corresponding ^{129}Xe NMR spectrum at 155 K. We attribute the difference to a much better communication among the various types of pores in MAS-7, i.e., good communication between micropores and mesopores and between neighboring mesopores though the pore wall that contains two different types of micropores. Our VT NMR result also suggests that our MAS-7 samples do not contain any impurities or other phases. For materials with mixed phases, sophisticated ^{129}Xe NMR spectra containing more than one resonance line were usually observed at low temperature.[34]

Microporosity in MAS-7. Our ^{129}Xe NMR results confirm the presence of micropores in MAS-7. This is consistent with earlier reports.[19−21] Moreover, the ^{129}Xe NMR provide a more detailed description of the microporosity in MAS-7. For example, two different types of micropores are present inside the pore walls of MAS-7, which could not be distinguished by other methods. To obtain an accurate determination of the diameter of micropores is very difficult. However, at least we can obtain an estimation of the sizes of micropores in MAS-7 through our ^{129}Xe NMR experiments. Coadsorption experiments reveal that the size of micropore I is about 0.74 nm, which is close to the channel size of zeolite beta. Recently, the catalytic probing reactions suggested that MAS-7 contains micropores with sizes of 0.74−0.87 nm.[21] The discrepancy is probably due to the fact that the catalytic reactions were carried out at a high temperature (573 K) while our ^{129}Xe NMR measurements were performed at room temperature. As mentioned above, precursors containing primary structure units of zeolite beta were prepared in the first step of the synthesis of MAS-7; we suspect that micropore I stems from this kind of primary structure units of zeolite beta.

The size of micropore II determined by ^{129}Xe NMR is in the range 0.44−0.49 nm, which is close the size of micropores in SBA-15.[41] In the syntheses of MAS-7 and SBA-15, the same template (tricopolymer surfactants, P123) was used. Thus, it can be expected that micropore II in MAS-7 is similar to that in SBA-15, which is likely generated by partial occlusion of triblock polymer chains into the mesoporous walls of MAS-7.

As revealed by our ^{129}Xe NMR experiments, although no direct communication is present between the two different types of micropores, there is a good communication between the two different types of micropores and mesopores in MAS-7. In addition, two neighboring mesopores are interconnected through the micropores. For example, the small molecules (such as xenon and water) adsorbed in one mesopore can pass through the pore wall that contains the two types of micropores to another neighboring mesopore. We suspect that the good communication network formed inside MAS-7 should be crucial to its excellent catalytic performance.

As compared with our ^{129}Xe NMR results, only one set of micropores (micropore I) was identified by catalytic probing reactions, and no detailed information is available about the communication among the various pore systems in MAS-7.[21]

Conclusions

Compared with other methods, such as TEM, ^{129}Xe NMR spectroscopy provides a more detailed description of the microporosity in MAS-7. Two different types of independent micropores (I and II) are present inside the mesoporous walls of MAS-7. On the basis of the coadsorption experiments of Xe and guest molecules with different sizes, we can estimate the size of micropores in MAS-7. Micropore I has a pore diameter

of about 0.74 nm, which is most likely formed by the primary structure units of zeolite beta, while the size of micropore II is in the range 0.44−0.49 nm, which may be generated from partial occlusion of triblock polymer chains into the mesoporous walls. VT ^{129}Xe NMR experiments indicate that xenon atoms in different adsorption states still undergo fast exchange with one another at low temperature, implying that there is a good communication among the various types of pores in MAS-7.

Acknowledgment. We thank Ms. Hanzhen Yuan and Mr. Wuyang Liu for NMR experiments. We are also grateful to the National Science Foundation (20173072, 20273082, and 10234070) and State Key Fundamental Research Program (2002ccc02200 and 2002CB713806) of China for financial support.

References and Notes

(1) Davis, M. E.; Saldarriaga, C.; Montes, C.; Garces, J.; Crowder, C. *Nature (London)* **1988**, *331*, 698.
(2) McCusker, L. B.; Baerlocher, C.; Jahn, A.; Bülow, M. *Zeolites* **1991**, *11*, 308.
(3) Kresge, C. T.; Leonowicz, M. E.; Roth, W. J.; Vartuli, J. C.; Beck, J. S. *Nature (London)* **1992**, *352*, 710.
(4) Beck, J. S.; Vartuli, J. C.; Roth, W. J.; Leonowicz, M. E.; Kresge, C. T.; Schmitt, K. D.; Chu, C. T.-W.; Olson, D. H.; Sheppard, E. W.; McCullen, S. B.; Higgins, J. B.; Schlenker, J. L. *J. Am. Chem. Soc.* **1992**, *114*, 10834.
(5) Corma, A. *Chem. Rev.* **1997**, *97*, 2373.
(6) Ryoo, R.; Kim, J. M.; Shin, C. H. *J. Phys. Chem.* **1996**, *100*, 17718.
(7) Kloestra, K. R.; Bekkum, H. V.; Jansen, J. C. *Chem. Comm.* **1997**, 2281.
(8) Yang, P.; Zhao, D.; Margolese, D.; Chmelka, B. F.; Stucky, G. D. *Nature (London)* **1998**, *396*, 152.
(9) Zhao, D.; Feng, J.; Huo, Q.; Melosh, N.; Fredrickso, G. H.; Chmelka, B. F.; Stucky, G. D. *Science* **1998**, *279*, 548.
(10) Kim, S. S.; Zhang, W.; Pinnawaia, T. J. *Science* **1998**, *282*, 1032.
(11) Yang, P.; Zhao, D.; Margolese, D.; Chmelka, B. F.; Stucky, G. D. *Chem. Mater.* **1999**, *11*, 2831.
(12) Mokaya, R. *Angew. Chem., Int. Ed.* **1999**, *38*, 2930.
(13) Hwang, L. M.; Guo, W. P.; Deng, P.; Xue, Z. Y.; Li, Q. Z. *J. Phys. Chem. B* **2000**, *104*, 2817.
(14) de Moor, P. E. A.; Beelen, T. P. M.; Santen, R. A. van; Tsuji, T.; Davis, M. E. *Chem. Mater.* **1999**, *11*, 36.
(15) de Moor, P. E. A.; Beelen, T. P. M.; Santen, R. A. van. *J. Phys. Chem. B* **1999**, *103*, 1639.
(16) Liu, Y.; Zhang, W.; Pinnavaia, T. J. *J. Am. Chem. Soc.* **2000**, *122*, 8791.
(17) Liu, Y.; Pinnavaia, T. J. *Chem. Mater.* **2002**, *14*, 3.
(18) Zhang, Z.; Han, Y.; Zhu, L.; Wang, R.; Yu, Y.; Qiu, S.; Zhao, D.; Xiao, F.-S. *Angew. Chem., Int. Ed.* **2001**, *40*, 1258.
(19) Han, Y.; Xiao, F.-S.; Wu, S.; Sun, Y.; Meng, X.; Li, D.; Lin, S.; Deng, F.; Ai, X. *J. Phys. Chem. B* **2001**, *105*, 7963.
(20) Liu, J.; Zhang, X.; Han, Y.; Xiao, F.-S. *Chem. Mater.* **2002**, *14*, 2536.
(21) Sun, Y.; Han, Y.; Yuan, L.; Ma, S.; Jiang, D.; Xiao, F.-S. *J. Phys. Chem. B* **2003**, *107*, 1853.
(22) Fraissard, J.; Ito, T. *Zeolites* **1988**, *8*, 350.
(23) Bonardet, J. L.; Fraissard, J.; Dedeon, A.; Springuel-Huet, M. A. *Catal. Rev.—Sci. Eng.* **1999**, *41*, 115.
(24) Demarquay, J.; Fraissard, J. *Chem. Phys. Lett.* **1987**, *136*, 314.
(25) Conner, W. C.; Weist, E. L.; Ito, T.; Fraissard, J. *J. Chem. Phys.* **1989**, *93*, 4138.
(26) Terskikh, V.; Mudrakovski, I.; Mastikhin, V. *J. Chem. Soc., Faraday Trans.* **1993**, *89*, 4239.
(27) Springuel-Huet, M.-A. Sun, K.; Fraissard, J. *Microporous Mesoporous Mater.* **1999**, *33*, 89.
(28) Springuel-Huet, M. A.; Bonardet, J. L.; Gédéon, A.; Yue, Y.; Fraissard, J. *Microporous Mesoporous Mater.* **2001**, *44−45*, 775.
(29) Pietrass, T.; Kneller, J. M.; Assink, R. A.; Anderson, M. T. *J. Phys. Chem. B* **1999**, *103*, 8837.
(30) Gedeon, A.; Ito, T.; Fraissard, J. *Zeolites* **1988**, *8*, 376.
(31) Ripmeester, J. A.; Ratchiffe, C. I. *Anal. Chim. Acta.* **1993**, *283*, 1103.
(32) Ripmeester, J. A.; Ratchiffe, C. I. *J. Phys. Chem.* **1990**, *94*, 7652.
(33) Cheung, T. T. P.; Fu, C. M.; Wharry, S. *J. Phys. Chem.* **1988**, *92*, 5170.
(34) Ryoo, R.; Pak, C.; Chmelka, B. F. *Zeolites* **1990**, *10*, 790.
(35) Zhou, Q.; Pang, W.; Qiu, S.; Jia, M. CN Patent ZL 93 1 17593.3, 1996.
(36) Zhou, Q.; Li, B.; Qiu, S.; Pang, W. *Chem. J. Chin. Univ.* **1999**, *20*, 693.
(37) Jameson, A. K.; Jameson, C. J.; Gutowsky, H. S. *J. Chem. Phys.* **1970**, *53*, 2310.
(38) Jameson, C. J.; Jameson, A. J.; Cohen, S. M. *J. Chem. Phys.* **1973**, *59*, 4540.
(39) *Cerius2*; Molecular Simulation/Biosysm Corp.: San Diego, CA, 1995.
(40) Etters, R. D.; Kaelberer, J. *Phys. Rev. A* **1975**, *11*, 1068; *J. Chem. Phys.* **1977,** *66*, 3233; *J. Chem. Phys.* **1977**, *66***,** 5112.
(41) Miyazawa, K.; Inagaki, S. *Chem. Commun.* **2000**, 2121.